Cabin Heat Thermal Management in Hybrid Vehicles using Model Predictive Control

Hasan Esen[1], Tsutomu Tashiro[2], Daniele Bernardini[3] and Alberto Bemporad[3]

***Abstract*— This paper describes a Model Predictive Control (MPC) design for the thermal management of cabin heat in Hybrid Electric Vehicles (HEVs). Due to the augmented complexity of the energy flow in recent energy-efficient vehicles in comparison to conventional vehicles, control degrees of freedom are increased, as many components can achieve the same functionality of heating up the cabin temperature. This paper proposes an MPC strategy to distribute the workload between available components in the vehicle, while achieving multiple objectives, such as fuel efficiency and heat-power reference tracking, and enforcing various constraints. First, a simplified linear dynamical model subject to linear time-varying (LTV) constraints is identified, based on high-fidelity simulations on a full nonlinear model. Then an MPC controller is designed to achieve multiple control objectives by manipulating different inputs. Simulation results indicate that the proposed approach is suitable for such multi-objective automotive control problems.**

I. INTRODUCTION

Energy management in vehicles means minimizing fuel consumption while satisfying driving and comfort requests of the driver. Conventional vehicles have only one energy source, the Internal Combustion Engine (ICE). However Hybrid Electric Vehicles (HEV) have two sources: an ICE and a high-voltage electric battery. Thus, the energy flow becomes more complicated in HEVs, which in return makes energy management a challenging problem.

There are several works considering energy management problems in HEVs. Many of them assume "ideal-world" conditions, i.e., take propulsion and electric energy flows into account, omitting thermal flow [1]–[9]. In this work, we focus on energy management in real-world, i.e., considering all three energy flow domains at the same time, see Figure 1. In ideal-world energy management, the engine is stopped frequently to save fuel. However, in real-world one must also consider using the engine to heat up the cabin, if needed. In [10] optimal thermal management for HEVs covers the minimization of energy consumption of the electrified HVAC auxiliaries, considering their maximum allowed temperature. The work in [11] underlines the importance of vehicle thermal management for HEVs/Plug-in HEVs. Rather than on control strategies, [11] focuses on weight reduction and aerodynamic improvements. The real-world optimal cabin-heat thermal management problem is tackled instead in [12], where the authors define optimal engine operating points, considering not only the fuel consumption map of the engine, but also the heat power transferred from the engine to the coolant. The approach of [12] is not model-based, and the optimization is done offline.

This paper presents a complete MPC design for solving the cabin heat thermal management problem in HEVs. With the tightening of requirements on engines and vehicles in terms of emissions, consumption and safety, the automotive industry is one of the fields where MPC techniques are rapidly becoming very popular [13]–[18]. The reason of such a strong interest in MPC is that it is suitable to fulfill such requirements, as most of them can be stated in the form of a constrained multiple input, multiple output control problem, and MPC provides a solution to this class of problems [19], [20]. The design described in this paper consists of three steps: first, identify simple linear prediction models, then formulate an MPC design with a proper selection of (time-varying) performance index and constraints, and finally validate the design by simulating the MPC controller in closed-loop with a high-fidelity nonlinear simulation model.

II. PROBLEM DEFINITION

The cabin can be heated up in a HEV vehicle either by removing heat-power from the engine coolant through the Heater Core (HC), or using electrical heaters, such as Positive Temperature Coefficient (PTC) heaters. The challenge in cabin heat thermal management is to manage the complex energy flows that are present, as described in Figure 1, and to satisfy different objectives simultaneously: provide the required thermal power, maintain the battery State of Charge (SoC) within given limits, and minimize fuel consumption.

We aim at formulating an MPC solution to thermal management for cabin heat control that minimizes fuel consumption by distributing the workload optimally between the heater core and an electrical heater (PTC), taking into account engine start/stop events. We assume that the resulting thermal management system operates independently of the electric management and the HV system. Hence, fuel consumption is optimized only by mixing the workloads of the heater core and of the electrical heater. To this end, three inputs are manipulated: (1) HC power u_1, (2) PTC power u_2, and (3) variation of engine power request u_3 with respect to baseline. The latter, filtered by a linear first-order model that accounts for dynamic effects such as coolant dynamics, mainly dictates bounds on the available heat-core power. The effect of such inputs in the overall thermal and electrical dynamics are derived in the next section, in which a simplified prediction model is obtained based on data from

[1]Technical Research Dept., DENSO AUTOMOTIVE Deutschland GmbH, Germany. E-mail: h.esen@denso-auto.de.
[2]Dept. of Mechanical Eng. for Transportation, Osaka Sangyo University, Japan. E-mail: tashiro@tm.osaka-sandai.ac.jp
[3]IMT Institute for Advanced Studies Lucca, Italy. E-mail: daniele.bernardini@imtlucca.it, alberto.bemporad@imtlucca.it

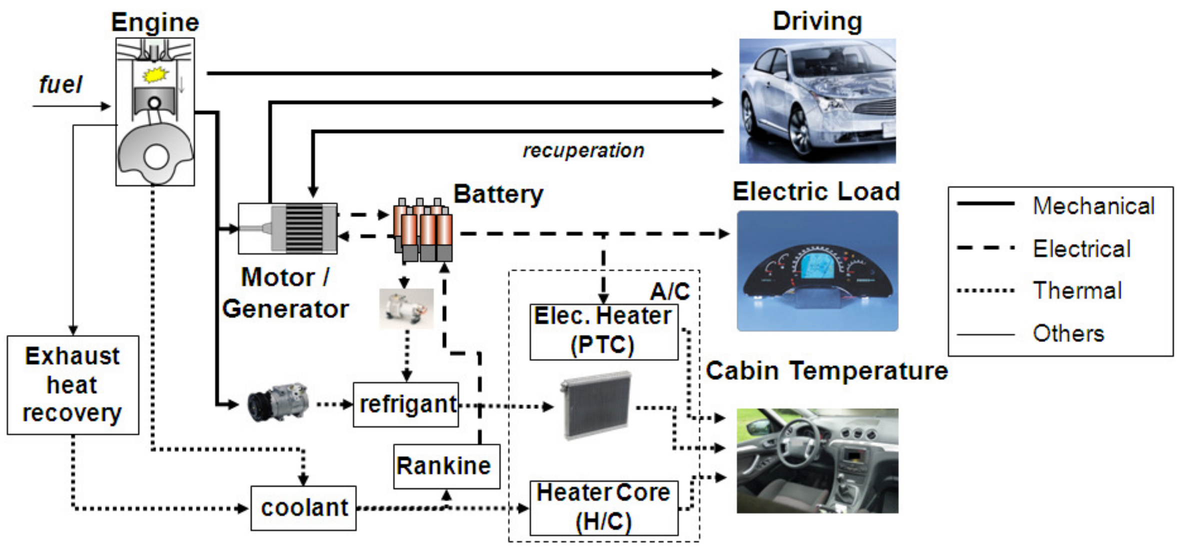

Fig. 1. Energy flows in hybrid-electric vehicles.

simulations for the only purpose of designing an effective linear time-varying MPC controller. The variables involved in the described dynamics are summarized in Table I.

III. Prediction Model

A. Thermal model

The total heat power $y_1(t)$ provided to cabin is given by the sum of powers provided by HC and PTC, i.e., $y_1(t) = u_1(t) + u_2(t)$. The thermal model considered for MPC design purposes is driven by the heat-core power input $u_1(t)$. It is assumed that the heater core power can be directly manipulated by the controller.

From the simulations reported in Figure 2, it is apparent a saturation of the heat-core power approximately at 5800 W. It is also noticed a transient behavior of the heat-core power $x_1(t)$ deliverable at full blower speed before reaching its steady-state. As the rise-time depends on the steady-state value, the dynamics are clearly nonlinear. Nonetheless, we approximate the dynamics of the maximum heat-core power $x_1(t)$ that can be delivered with full blower level as the first-order linear system

$$x_1(t) = \frac{1}{1+\tau_1 s}(u_3(t) + v_3(t)) \tag{1}$$

via nonlinear scalar optimization of the time constant τ_1. In (1), $u_3(t)+v_3(t)$ is the actual engine power request, being $v_3(t)$ a measured disturbance corresponding to the baseline engine power request.

B. Electrical model

A dynamical model of the battery is needed for imposing constraints on the SoC of the battery, $x_2(t)$, and to track a desired SoC set-point. We model the SoC dynamics as an integrator with state $x_2(t)$ driven by the total electrical power $z_2(t)$ and the recharging effect $z_1(t)$ of the engine on the battery:

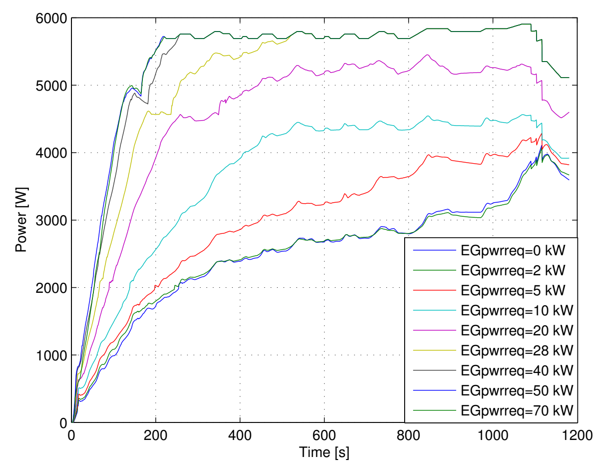

Fig. 2. Time evolution of heat-core power at full blower level for different engine power requests.

$$\frac{dx_2(t)}{dt} = k_2 z_2(t) + z_1(t), \tag{2}$$

where

$$z_1(t) = k_1 v_1(t)(u_3(t) + v_3(t)), \tag{3}$$

$v_1(t)$ is a measured disturbance denoting engine ON ($v_1(t) = 1$) or OFF ($v_1(t) = 0$), $z_2(t)$ is the total electrical power

$$z_2(t) = u_2(t) + v_2(t), \tag{4}$$

$v_2(t)$ is the total electrical power (voltage by current) minus the power drained by the PTC at time t, and k_1, k_2 are suitable constants obtained by fitting simulation data.

We denote by $y_2(t) = x_2(t)$ the SoC, that is the output of model (2). The quantity $k_1 v_1(t)(u_3(t) + v_3(t))$ in (3) takes into account that the battery is recharged by increasing the engine power request. We assume that the PTC electrical

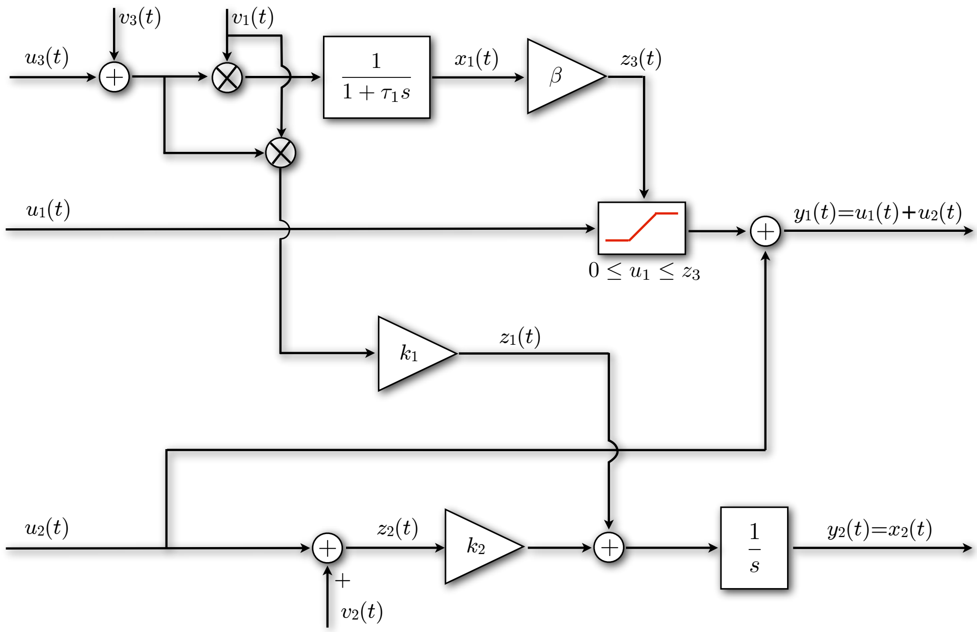

Fig. 3. Block diagram of prediction model.

TABLE I
VARIABLES RELEVANT TO THE MPC PREDICTION MODEL

Description	**Model variable**
Inputs	
Thermal power delivered by HC	u_1
Thermal power delivered by PTC	u_2
Variation of engine power request	u_3
States	
Filtered max heat-core power at full blower level	x_1
Battery state of charge	x_2
Outputs	
Total heat power	$y_1 = u_1 + u_2$
Battery state of charge	$y_2 = x_2$
Measured disturbances	
Engine ON/OFF request	v_1
Total electrical power minus PTC	v_2
Engine baseline power request	v_3
Aux. variables	
Battery charge due to engine power	z_1
Total electrical power	z_2
Max heat-core power at full blower level	z_3
Set-points	
Total heat power request	r_1
Desired state of charge	r_2
Desired additional power request	r_3

power signal $u_2(t)$ is also equal to the heat power supplied by the PTC to the cabin. The block diagram of the overall simplified prediction model is shown in Figure 3.

IV. CONSTRAINED OPTIMAL CONTROL PROBLEM FORMULATION

A. *Set-points and cost function*

Let $r_1(t)$ be the desired set-point on total heat power $y_1(t)$ and $r_2(t)$ the desired battery level for $y_2(t)$. An engine characteristics map is used to determine the optimal set-point $r_3(t)$ for additional power requests $u_3(t)$, aiming to move the engine Operating Point (OP) by minimizing marginal fuel consumption rates. We consider the general case where the MPC controller can request both positive and negative additional power. Negative additional power can be commanded in order to shift part of the power request from the engine to the electrical motor and the generator, with the goal of reducing fuel consumption and, at the same time, tracking the desired set-point on the battery state of charge.

To determine the set-point $r_3(t)$ in real-time, an appropriate simple selection algorithm (omitted in this paper) is run at each time step t based on the current heat-core power and battery SoC, and on optimal torque functions f_T^+, f_T^- computed offline describing, respectively, optimal positive and negative torque variations. These are defined as

$$\begin{aligned} f_T^+ &= \text{arg min}_{T_2} K^{-1} \frac{F(\omega_2, T_2) - F(\omega_1, T_1)}{\omega_1 (T_2 - T_1)} \\ &\text{s.t.} \quad 0 < T_2 - T_1 \le \Delta T_{\max} \end{aligned} \tag{5}$$

$$\begin{aligned} f_T^- &= \text{arg max}_{T_2} K^{-1} \frac{F(\omega_2, T_2) - F(\omega_1, T_1)}{\omega_1 (T_2 - T_1)} \\ &\text{s.t.} \quad -\Delta T_{\max} \le T_2 - T_1 < 0 \end{aligned} \tag{6}$$

where $K = \frac{\pi}{30} \cdot 10^{-3}$, $F(\omega, T)$ is the engine fuel consumption rate mapping [g/h] at a given engine OP (ω, T), the pair (ω_1, T_1) is the current engine OP, the pair (ω_2, T_2) is the optimal engine OP, and the value $\Delta T_{\max} = 30$ Nm

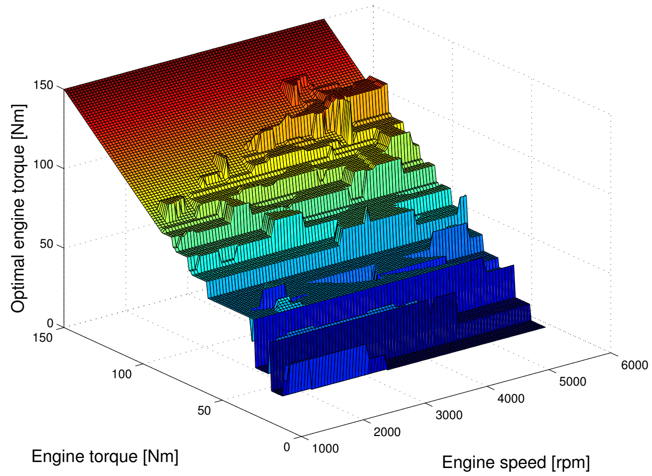

Fig. 4. Optimal engine torque for different engine torque/speed pairs ($r_3(t) \geq 0$).

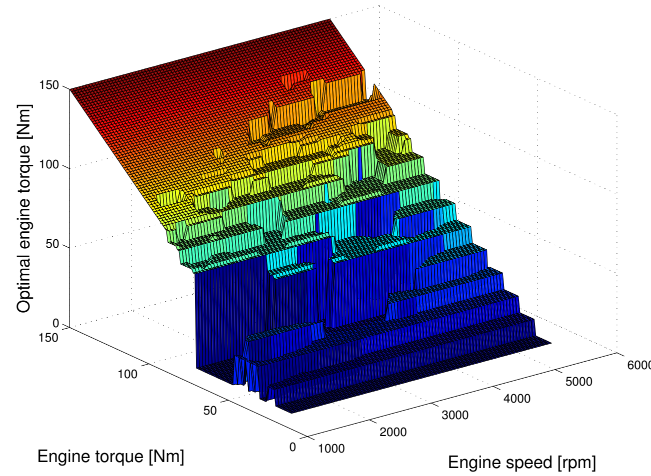

Fig. 5. Optimal engine torque for different engine torque/speed pairs ($r_3(t) \leq 0$).

describes the maximum allowed variation from the current engine torque T_1. Problems (5)-(6) are solved offline for the whole range of admissible engine speed and torque values, considering constant engine speed ($\omega_1 = \omega_2$), and approximated by lookup tables for real-time implementation. The optimal engine OP maps resulting by the solution of (5)-(6) and the related torque values are shown in Figures 4 and 5.

The main idea behind the selection of the incremental engine power request $r_3(t)$ is that power request is increased ($r_3(t) > 0$) if the SoC $y_1(t)$ is relatively low or more heat-core power is needed, while it is decreased otherwise ($r_3(t) < 0$).

The overall stage cost $\ell(y(t), u(t))$ to be minimized in the MPC problem is defined as

$$\begin{aligned}\ell(y(t), u(t)) = {} & \rho_1(y_1(t) - r_1(t))^2 + \rho_2(t)(y_2(t) - r_2(t))^2 \\ & + \ \rho_3 u_2^2(t) + \rho_4(u_3(t) - r_3(t))^2 \\ & + \ \sigma_1 \Delta u_1^2(t) + \sigma_2 \Delta u_2^2(t) + \sigma_3 \Delta u_3^2(t), \quad (7)\end{aligned}$$

where ρ_1, ρ_3, ρ_4, σ_1, σ_2, σ_3 are constant weights, and $\Delta u_j(t) = u_j(t) - u_j(t-1)$ denote input increments, for all $j \in \{1, 2, 3\}$. The time-varying weight $\rho_2(t)$ on SoC deviations from the desired set-point allows one to admit larger variations of the battery state of charge at the beginning of the drive cycle and penalize deviation towards the end of the cycle.

B. Constraints

The input $u_1(t)$ must be generated under the constraint

$$u_1(t) \leq z_3(t),$$

where the upper bound $z_3(t) \triangleq \beta x_1(t)$ corresponds to a conservative ($0 < \beta < 1$) approximation of the maximum heat-core power $x_1(t)$ at full blower level. The thermal power $u_2(t)$ produced by PTC is subject instead to the constraint

$$0 \leq u_2(t) \leq PTC_{\max}(t), \quad (8)$$

The maximum available PTC power $PTC_{\max}(t)$ is defined at each time step t as a function of the air flow rate from blower and the air temperature at the heater core outlet. Since we treat the heat-core power as a manipulated input, $u_1(t)$, there is a dynamic correlation between $u_1(t)$ and $PTC_{\max}(t)$, which is accounted for in the prediction model. We modified the upper bound on PTC power request to reflect such correlation, resulting in the time-varying constraint (8).

The variation $u_3(t)$ of engine power request is constrained as

$$dEG_{\text{low}} \leq u_3(t) \leq dEG_{\text{up}}. \quad (9)$$

In order to allow negative additional power requests, the bounds on $u_3(t)$ are defined as

$$\begin{aligned} dEG_{\text{low}} &= \min\{0, \max\{r_3(t), v_3(t)\}\} \\ dEG_{\text{up}} &= v_{3,\max} - v_3(t) \end{aligned} \quad (10)$$

where $r_3(t)$ is the set-point on additional power request and $v_{3,\max}$ is the maximum engine power request. Moreover, the SoC $x_2(t)$ must satisfy the constraint

$$0.35 \leq x_2(t) \leq 0.75 \quad (11)$$

V. MPC Formulation

The control problem at time t can be stated as follows. Given the current on/off status $v_1(t)$ of the engine, the baseline electrical consumption $v_2(t)$, the engine baseline power request $v_3(t)$, and some other engine and heat-core related measurements, select the manipulated variables HC power $u_1(t)$, PTC heat power $u_2(t)$, incremental engine power request $u_3(t)$ so that the best compromise between the following three objectives is achieved: $y_1(t) = r_1(t)$ (desired total heat power), $y_2(t) = r_2(t)$ (desired battery level), and fuel consumption is minimized.

By discretizing the system models derived in Section III with sampling time T_s, we obtain the following prediction model at time t for each prediction step $t+k$:

$$x_1(t+k+1) = e^{-\frac{T_s}{\tau_1}} x_1(t+k) + (1-e^{-\frac{T_s}{\tau_1}}) v_1(t)(u_3(t+k)+v_3(t)) \tag{12a}$$

$$x_2(t+k+1) = x_2(t+k) + T_s z_1(t+k) + T_s k_2 z_2(t+k) \tag{12b}$$

$$y_1(t+k) = u_1(t+k) + u_2(t+k) \tag{12c}$$

$$y_2(t+k) = x_2(t+k) \tag{12d}$$

$$z_1(t+k) = k_1 v_1(t) u_3(t+k) \tag{12e}$$

$$z_2(t+k) = u_2(t+k) + v_2(t) \tag{12f}$$

$$z_3(t+k) = \beta x_1(t+k) \tag{12g}$$

subject to the constraints

$$0 \leq u_1(t+k) \leq z_3(t+k) \tag{13a}$$

$$0 \leq u_2(t+k) \leq PTC_{\max}(t) \tag{13b}$$

$$dEG_{\text{low}} \leq u_3(t+k) \leq dEG_{\text{up}} \tag{13c}$$

$$0.35 \leq x_2(t+k) \leq 0.75 \tag{13d}$$

The performance index $J(t)$ to be minimized at each time t is defined over a prediction horizon of N steps in accordance with (7):

$$\begin{aligned} J(t) = & \sum_{k=0}^{N-1} \rho_1(y_1(t+k) - r_1(t))^2 \\ + & \rho_2(t)(y_2(t+k) - r_2(t))^2 \\ + & \rho_3 u_2^2(t+k) \\ + & \rho_4(u_3(t+k) - r_3(t))^2 \\ + & \textstyle\sum_{j=1}^{3} \sigma_j \Delta u_j^2(t+k) \end{aligned} \tag{14}$$

A. MPC Algorithm

At a given sampling time t, given the current estimated maximum heat-core power at full blower level $x_1(t)$, the current SoC $x_2(t)$, the current engine ON/OFF status $v_1(t)$, electrical power consumption $v_2(t)$, engine baseline power request v_3, weight $\rho_2(t)$, and set-points $r_1(t)$, $r_2(t)$, $r_3(t)$, we solve the following MPC problem via standard quadratic programming (QP):

$$\min_{U} \quad J(t) \tag{15a}$$

$$\text{s.t.} \quad \text{Eqs. (12), (13)}, \ \forall k = 0, \ldots, N-1, \tag{15b}$$

$$u_j(t+k) = u_j(t+N_u-1), \quad \forall k = N_u, \ldots, N-1, \forall j = 1,2,3, \tag{15c}$$

where $U = \{u_1(t+k), u_2(t+k), u_3(t+k)\}_{k=0}^{N_u-1}$ and N_u is the control horizon, $N_u \leq N$.

The constraints on the battery state of charge $x_2(t)$ are implemented as soft constraints to prevent the possible infeasibility of the MPC problem (15) at some time t. Since future set-points on total heat power $r_1(t+k)$, desired battery level $r_2(t+k)$ and additional power request $r_3(t+k)$ are assumed to be not known in advance, we simply keep them constant in prediction, $r_i(t+k) = r_i(t)$, $\forall k = 0, \ldots, N-1$, $i = 1,2,3$.

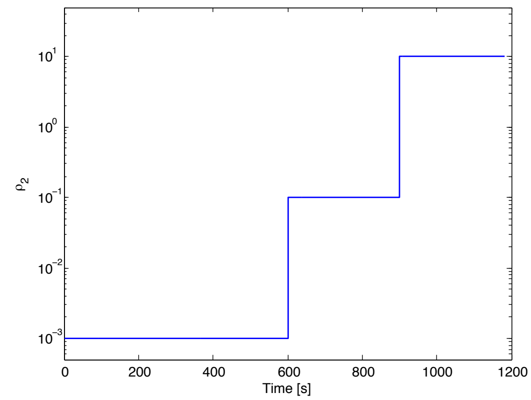

Fig. 6. Time-varying weight $\rho_2(t)$ on SoC deviations from desired set-point.

Note that $r_1(t)$ and $r_2(t)$ are user-defined signals, while $r_3(t)$ is dynamically computed as described in Section IV-A.

The MPC problem (15) is linear time-varying, in that signal $v_1(t) \in \{0, 1\}$ and $v_2(t) \in \mathbb{R}$ may change the dynamic equations from one time step to another, the upper bound on the available PTC power depends on t, and the weight on battery SoC tracking is also time-varying.

VI. Simulation Results

The developed controller is tested in a HEV simulation model under MATLAB/Simulink. The simulation conditions to test the developed controller are set as follows: New European Driving Cycle (NEDC) as the drive cycle, ambient temperature 5°C, cold-start, A/C on, initial SoC at 60%. The time-varying weight $\rho_2(t)$ is defined as

$$\rho_2(t) = \begin{cases} 0.001 & \text{if } t \leq 600 \\ 0.1 & \text{if } 600 < t \leq 900 \\ 10 & \text{otherwise} \end{cases} \tag{16}$$

and it is shown in Figure 6. The reference heat-power trajectory is depicted in Figure 7 (dotted black line), while the reference battery SoC is $r_2(t) \equiv x_2(0) = 0.6$.

As illustrated in Figure 7, MPC achieves a good tracking of the given heat-core power reference $r_1(t)$. Figure 8 indicates that the battery SoC level $x_2(t)$ is always maintained within its limits, and the final SoC value is very close to the initial value. Simulation results have shown remarkable improvements with respect to the reference baseline controller also regarding fuel consumption, up to 3%.

VII. Conclusion

In this work a linear time-varying MPC formulation for HEV thermal management of cabin heat has been devised. Presented results have shown improvements (up to 3% fuel savings) with respect to a reference baseline controller, therefore demonstrating the benefits of MPC. The proposed implementation grants a high degree of reusability and maintainability: for example, it is easy to change bounds on input or state variables, modify dynamics equations, or revise the cost function after having observed changes in the model.

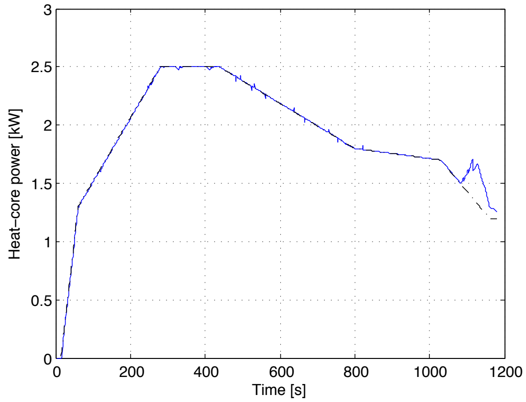

Fig. 7. Heat-core power tracking with MPC.

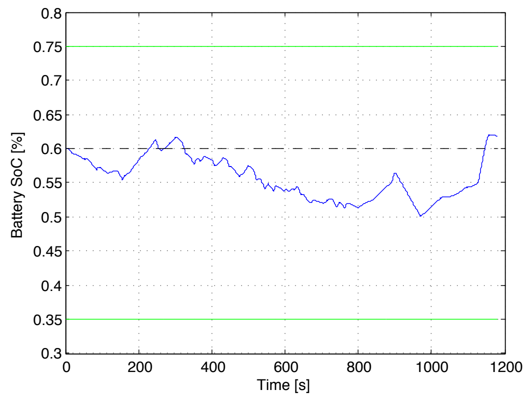

Fig. 8. Battery State of Charge tracking with MPC.

References

[1] M. Debertand, G. Colin, Y. Chamaillard, L. Guzzella, A. Ketfi-Cherif, and B. Bellicaud, "Predictive energy management for hybrid electric vehicles – prediction horizon and battery capacity sensitivity," in *Proc. IFAC Symposium on Advances in Automotive Control*, Munich, Germany, 2010.

[2] D. Kum, H. Peng, and N. Bucknor, "Optimal control of plug-in hevs for fuel economy under various travel distances," in *Proc. IFAC Symposium on Advances in Automotive Control*, Munich, Germany, 2010, pp. 258–263.

[3] T. van Keulen anbd B. de Jager, J. Kessels, and M. Steinbuch, "Energy management in hybrid electric vehicles: Benefit of prediction," in *Proc. IFAC Symposium on Advances in Automotive Control*, Munich, Germany, 2010.

[4] M. Kamal, M. M. abd J. Murata, and T. Kawabe, "Ecological driving based on preceding vehicle prediction using MPC," in *Proc. 18th IFAC World Congress*, Milano, Italy, 2011, pp. 3843–3848.

[5] M. Bichi, G. Ripaccioli, S. D. Cairano, D. Bernardini, A. Bemporad, and I. Kolmanovsky, "Stochastic model predictive control with driver behavior learning for improved powertrain control," in *Proc. 49th IEEE Conf. on Decision and Control*, Atlanta, GA, USA, 2010, pp. 6077–6082.

[6] T. Kim, K. Manzie, and R. Sharma, "Two-stage optimal control of a parallel hybrid vehicle with traffic preview," in *Proc. 18th IFAC World Congress*, Milano, Italy, 2011, pp. 2115–2120.

[7] R. Beck, A. Bollig, and D. Abel, "Comparison of two real-time predictive strategies for the optimal energy management of a hybrid electric vehicle," *Oil & Gas Science and Technology*, vol. 62, no. 4, pp. 635–643, 2007.

[8] S. Stockar, V. Marano, M. Canova, G. Rizzoni, and L. Guzzella, "Energy-optimal control of plug-in hybrid electric vehicles for real-world driving cycles," *IEEE Transactions on Vehicular Technology*, vol. 60, no. 7, pp. 2949–2962, 2011.

[9] M. Kamal, M. Mukai, J. Murata, and T. Kawabe, "Development of ecological driving assist system model predictive approach in vehicle control," in *16th ITS World Congress and Exhibition on Intelligent Transport Systems and Services*, Stockholm, Sweden, 2009.

[10] F. Kitanoski and A. Hofer, "A contribution to energy optimal thermal management for vehicles," in *Proc. IFAC Symposium on Advances in Automotive Control*, Munich, Germany, 2010, pp. 87–92.

[11] K. Bennion and M. Thornton, "Integrated vehicle thermal management for advanced vehicle propulsion technologies," *Proc. SAE 2010 World Congress*, p. 7, 2010.

[12] T. Tashiro, T. Okamoto, and T. Yagi, "Energy management on hybrid vehicle covering cabin heat power from engine," in *Proc. 11th International Symposium on Advanced Vehicle Control (AVEC '12)*, Seoul, Korea, 2012.

[13] L. del Re, P. Ortner, and D. Alberer, "Chances and challenges in automotive predictive control," in *Automotive Model Predictive Control*. Springer, 2010, pp. 1–22.

[14] S. Di Cairano, A. Bemporad, I. Kolmanovsky, and D. Hrovat, "Model predictive control of magnetically actuated mass spring dampers for automotive applications," *Int. Journal of Control*, vol. 80, no. 11, pp. 1701–1716, 2007.

[15] F. Borrelli, A. Bemporad, M. Fodor, and D. Hrovat, "An MPC/hybrid system approach to traction control," *IEEE Trans. Contr. Systems Technology*, vol. 14, no. 3, pp. 541–552, May 2006.

[16] N. Giorgetti, A. Bemporad, H. Tseng, and D. Hrovat, "Hybrid model predictive control application towards optimal semi-active suspension," *Int. Journal of Control*, vol. 79, no. 5, pp. 521–533, 2006.

[17] P. Falcone, F. Borrelli, J. Asgari, H. Tseng, and D. Hrovat, "Predictive active steering control for autonomous vehicle systems," *IEEE Trans. Contr. Systems Technology*, vol. 15, no. 3, pp. 566–580, 2007.

[18] S. Di Cairano, D. Yanakiev, A. Bemporad, I. Kolmanovsky, and D. Hrovat, "Model predictive idle speed control: Design, analysis, and experimental evaluation," *IEEE Trans. Contr. Systems Technology*, vol. 20, no. 1, pp. 84–97, 2012.

[19] S. Qin and T. Badgwell, "A survey of industrial model predictive control technology," *Control Engineering Practice*, vol. 11, pp. 733–764, 2003.

[20] A. Bemporad, "Model-based predictive control design: New trends and tools," in *Proc. 45th IEEE Conf. on Decision and Control*, San Diego, CA, 2006, pp. 6678–6683.